Article

Copper(I)/S Reversible Reactions Leading to an End-On Bound Dicopper(II) Disulfide Complex: Nucleophilic Reactivity and Analogies to Copper–Dioxygen Chemistry

Debabrata Maiti, Julia S. Woertink, Michael A. Vance, Ashley E. Milligan, Amy A. Narducci Sarjeant, Edward I. Solomon, and Kenneth D. Karlin

J. Am. Chem. Soc., **2007**, 129 (28), 8882-8892• DOI: 10.1021/ja071968z • Publication Date (Web): 26 June 2007

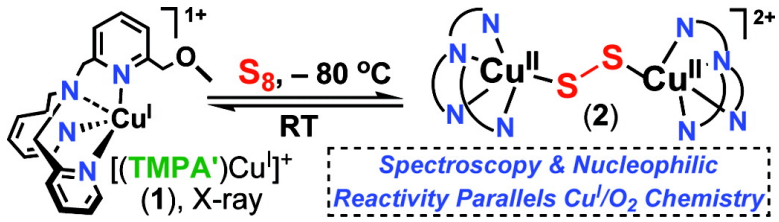

More About This Article

Additional resources and features associated with this article are available within the HTML version:

- Supporting Information
- Links to the 9 articles that cite this article, as of the time of this article download
- Access to high resolution figures
- Links to articles and content related to this article
- Copyright permission to reproduce figures and/or text from this article

View the Full Text HTML

J|A|C|S
ARTICLES
Published on Web 06/26/2007

Copper(I)/S_8 Reversible Reactions Leading to an End-On Bound Dicopper(II) Disulfide Complex: Nucleophilic Reactivity and Analogies to Copper−Dioxygen Chemistry

Debabrata Maiti,[†] Julia S. Woertink,[‡] Michael A. Vance,[‡] Ashley E. Milligan,[‡] Amy A. Narducci Sarjeant,[†] Edward I. Solomon,[‡] and Kenneth D. Karlin*,[†]

Contribution from the Department of Chemistry, Johns Hopkins University, Baltimore, Maryland 21218, and Department of Chemistry, Stanford University, Stanford, California 94305

Received March 30, 2007; E-mail: karlin@jhu.edu

Abstract: Elemental sulfur (S_8) reacts reversibly with the copper(I) complex [(**TMPA′**)Cu^I]$^+$ (**1**), where **TMPA′** is a **TMPA** (tris(2-pyridylmethyl)amine) analogue with a 6-CH_2OCH_3 substituent on one pyridyl ligand arm, affording a spectroscopically pure end-on bound disulfido−dicopper(II) complex [{(**TMPA′**)Cu^{II}}$_2$(μ-1,2-S_2^{2-})]$^{2+}$ (**2**) {$\nu_{(S-S)} = 492$ cm^{-1}; $\nu_{(Cu-S)sym} = 309$ cm^{-1}}; by contrast, [(**TMPA**)Cu^I(CH_3CN)]$^+$ (**3**)/S_8 chemistry produces an equilibrium mixture of at least three complexes. The reaction of excess PPh_3 with **2** leads to formal "release" of zerovalent sulfur and reduction of copper ion to give the corresponding complex [(**TMPA′**)Cu^I(PPh_3)]$^+$ (**11**) along with S=PPh_3 as products. Dioxygen displaces the disulfur moiety from **2** to produce the end-on Cu_2O_2 complex, [{(**TMPA′**)Cu^{II}}$_2$(μ-1,2-O_2^{2-})]$^{2+}$ (**9**). Addition of the tetradentate ligand **TMPA** to **2** generates the apparently more thermodynamically stable [{(**TMPA**)Cu^{II}}$_2$(μ-1,2-S_2^{2-})]$^{2+}$ (**4**) and expected mixture of other species. Bubbling **2** with CO leads to the formation of the carbonyl adduct [(**TMPA′**)Cu^I(CO)]$^+$ (**8**). Carbonylation/sulfur-release/CO-removal cycles can be repeated several times. Sulfur atom transfer from **2** also occurs in a near quantitative manner when it is treated with 2,6-dimethylphenyl isocyanide (ArNC), leading to the corresponding isothiocyanate (ArNCS) and [(**TMPA′**)Cu^I(CNAr)]$^+$ (**12**). Complex **2** readily reacts with $PhCH_2Br$: [{(**TMPA′**)Cu^{II}}$_2$(μ-1,2-S_2^{2-})]$^{2+}$ (**2**) + 2 $PhCH_2Br$ → [{(**TMPA′**)Cu^{II}(Br)}$_2$]$^{2+}$ (**6**) + $PhCH_2SSCH_2Ph$. The unprecedented substrate reactivity studies reveal that end-on bound μ-1,2-disulfide−dicopper(II) complex **2** provides a nucleophilic S_2^{2-} moiety, in striking contrast to the electrophilic behavior of a recently described side-on bound μ-η^2:η^2-disulfido−dicopper(II) complex, [{(N_3)Cu^{II}}$_2$(μ-η^2:η^2-S_2^{2-})]$^{2+}$ (**5**) with tridentate N_3 ligand. The investigation thus reveals striking analogies of copper/sulfur and copper/dioxygen chemistries, with regard to structure type formation and specific substrate reactivity patterns.

Introduction

While copper chalcogenide compounds are of interest in structural, synthetic, and materials chemistry,[1−4] recent attention has included efforts leading to Cu−S assemblies that possess nitrogen containing chelates and sulfide (S^{2-}) or disulfide (e.g., S_2^{2-}) bridging moieties.[5−15] Such chemistry has in part been inspired by the occurrence of a (histidine)$_7$Cu$_4$(μ_4-S) cluster (referred to as Cu_Z) at the active site of nitrous oxide reductase (N_2OR) and copper(I)−sulfido chemistry in carbon monoxide dehydrogenase.[16−18] N_2OR catalyzes the final step in bacterial denitrification, $N_2O + 2e^- + 2H^+ \rightarrow H_2O + N_2$[9,19−22] and plays

[†] Johns Hopkins University.
[‡] Stanford University.

(1) Dance, I.; Fisher, K. *Prog. Inorg. Chem.* **1994**, *41*, 637−803.
(2) Steudel, Y.; Wong, M. W.; Steudel, R. *Eur. J. Inorg. Chem.* **2005**, 2514−2525.
(3) Dehnen, S.; Eichhofer, A.; Fenske, D. *Eur. J. Inorg. Chem.* **2002**, 279−317.
(4) Donahue, J. P. *Chem. Rev.* **2006**, *106*, 4747−4783.
(5) Fujisawa, K.; Morooka, Y.; Kitajima, N. *J Chem. Soc., Chem. Commun.* **1994**, 623−624.
(6) Helton, M. E.; Chen, P.; Paul, P. P.; Tyeklár, Z.; Sommer, R. D.; Zhakarov, L. N.; Rheingold, A. L.; Solomon, E. I.; Karlin, K. D. *J. Am. Chem. Soc.* **2003**, *125*, 1160−1161.
(7) Helton, M. E.; Maiti, D.; Zakharov, L. N.; Rheingold, A. L.; Porco, J. A.; Karlin, K. D. *Angew. Chem., Int. Ed.* **2006**, *45*, 1138−1141.
(8) Lee, Y.; Sarjeant, A. A. N.; Karlin, K. D. *Chem. Commun.* **2006**, 621−623.
(9) Lee, D.-H.; Mondal, B.; Karlin, K. D. NO and N_2O Binding and Reduction. In *Activation of Small Molecules: Organometallic and Bioinorganic Perspectives;* Tolman, W. B., Ed.; Wiley-VCH: New York, 2006; pp 43−79.
(10) Brown, E. C.; Aboelella, N. W.; Reynolds, A. M.; Aullon, G.; Alvarez, S.; Tolman, W. B. *Inorg. Chem.* **2004**, *43*, 3335−3337.
(11) Chen, P.; Fujisawa, K.; Helton, M. E.; Karlin, K. D.; Solomon, E. I. *J. Am. Chem. Soc.* **2003**, *125*, 6394−6408.
(12) Brown, E. C.; York, J. T.; Antholine, W. E.; Ruiz, E.; Alvarez, S.; Tolman, W. B. *J. Am. Chem. Soc.* **2005**, *127*, 13752−13753.
(13) York, J. T.; Brown, E. C.; Tolman, W. B. *Angew. Chem., Int. Ed.* **2005**, *44*, 7745−7748.
(14) Tolman, W. B. *J. Biol. Inorg. Chem.* **2006**, *11*, 261−271.
(15) Brown, E. C.; Bar-Nahum, I.; York, J. T.; Aboelella, N. W.; Tolman, W. B. *Inorg. Chem.* **2007**, *46*, 486−496.
(16) Gourlay, C.; Nielsen, D. J.; White, J. M.; Knottenbelt, S. Z.; Kirk, M. L.; Young, C. G. *J. Am. Chem. Soc.* **2006**, *128*, 2164−2165.
(17) Hofmann, M.; Kassube, J.; Graf, T. *J. Biol. Inorg. Chem.* **2005**, *10*, 490−495.
(18) Resch, M.; Dobbek, H.; Meyer, O. *J. Biol. Inorg. Chem.* **2005**, *10*, 518−528.
(19) Gorelsky, S. I.; Ghosh, S.; Solomon, E. I. *J. Am. Chem. Soc.* **2006**, *128*, 278−290.
(20) Chen, P.; Gorelsky, S. I.; Ghosh, S.; Solomon, E. I. *Angew. Chem., Int. Ed.* **2004**, *43*, 4132−4140.
(21) Paraskevopoulos, K.; Antonyuk, S. V.; Sawers, R. G.; Eady, R. R.; Hasnain, S. S. *J. Mol. Biol.* **2006**, *362*, 55−65.

10.1021/ja071968z CCC: $37.00

Chart 1

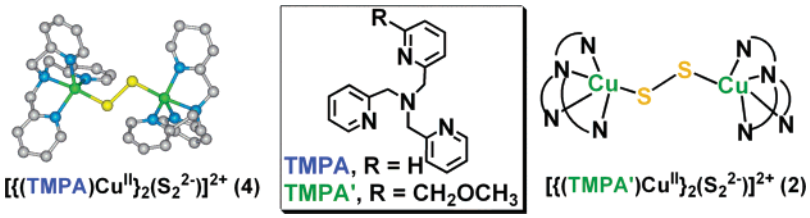

a critical environmental role by preventing release of greenhouse gas nitrous oxide. This reduction of N_2O is thermodynamically favorable, but in homogeneous chemical systems, its extreme kinetic inertness normally leads to the requirement of a very active transition-metal complex to effect its reduction/transformation.[9,23,24] In N_2OR and at Cu_Z, experimental and theoretical studies lead to the conclusion that a fully reduced $(Cu^I)_4$ cluster is the activated form ready for N_2O interaction/reduction;[20,25] more oxidized forms have been identified and may be catalytically relevant.[19,20,25,26]

Soft, abiological ligands (e.g., phosphines) are known[3,27,28] to stabilize Cu^I−sulfido species, but relatively little is known about copper−sulfur chemistry with N-donor ligands. As such, our group and that of Tolman have set out to explore fundamental aspects of copper−sulfur complexes incorporating N-donor ligand to elucidate synthetic methodologies, deduce structures and spectroscopy/bonding aspects, and explore reactivity patterns.[6−15]

In this report, we describe the chemistry of a new disulfido−dicopper(II) complex, $[\{(\mathbf{TMPA'})Cu^{II}\}_2(\mu\text{-}1,2\text{-}S_2^{2-})]^{2+}$ (**2**), formed by the reaction of elemental sulfur (S_8) with $[(\mathbf{TMPA'})Cu^I]^+$ (**1**) (Chart 1). Ligand **TMPA′** is a tripodal N_4 tetradentate ligand, a close analogue of **TMPA** {≡(tris(2-pyridyl)methylamine}, but with a 6-CH_2OCH_3 substituent on one pyridyl ligand arm (Chart 1). While we previously structurally characterized $[\{(\mathbf{TMPA})Cu^{II}\}_2(\mu\text{-}1,2\text{-}S_2^{2-})]^{2+}$ (**4**) (Chart 1), it could only be isolated in small quantities and exists in solution as an equilibrium mixture,[6,11] as described in more detail in this present report. However, resonance Raman (rR) spectroscopic studies revealed that a 568 nm absorption corresponds to the X-ray structure (that shown in Chart 1).[6,11] Here, by contrast, our ligand modification (**TMPA′**) affords a spectroscopically pure compound **2**, as described below. We have thus been able to carry out substrate reactivity studies that for the first time elucidate the nature of the (di)sulfur moiety present in such a structural configuration. The results reveal that the end-on bound μ-1,2-disulfido−dicopper(II) complex **2** provides a nucleophilic S_2^{2-} moiety, in striking contrast to the electrophilic behavior of a recently described side-on bound μ-η^2:η^2-disulfido−dicopper(II) complex with tridentate ligand, $[\{(N_3)Cu^{II}\}_2(\mu\text{-}\eta^2\text{:}\eta^2\text{-}S_2^{2-})]^{2+}$ (**5**) (Chart 2) (N_3 = *N*,*N*-bis{2-[2-(*N*′,*N*′-4-dimethylamino)-pyridyl]ethyl}methylamine).[7] Furthermore, the present investigation reveals striking analogies to dioxygen−copper chemistry and substrate reactivity of peroxide-bound dicopper(II) complexes.[11]

Experimental Section

Materials and Methods. Unless otherwise stated, all solvents and chemicals used were of commercially available analytical grade. Dioxygen was dried by passing through a short column of supported P_4O_{10} (Aquasorb, Mallinckrodt). Tetrahydrofuran (THF) and pentane were used after passing them through a 60-cm-long column of activated alumina (Innovative Technologies, Inc.) under argon. Preparation and handling of air-sensitive compounds were performed under an argon atmosphere using standard Schlenk techniques or in an MBraun Labmaster 130 inert atmosphere (<1 ppm O_2, <1 ppm H_2O) drybox filled with nitrogen. Deoxygenation of solvents was effected by either repeated freeze/pump/thaw cycles or bubbling with argon for 30−45 min. Elemental analyses were performed by Desert Analytics. ^{1}H NMR spectra were measured on a Bruker 400 MHz spectrometer. Chemical shifts were reported as δ values relative to an internal standard (Me_4-Si), and the residual solvent proton peak. UV−vis spectra were recorded with either a Cary-50 Bio spectrophotometer equipped with a fiber optic coupler (Varian, Inc.) and a fiber optic dip probe (Hellma: 661.302-QX-UV 2 mm for low temperature) or a Hewlett-Packard model 8453A

Chart 2

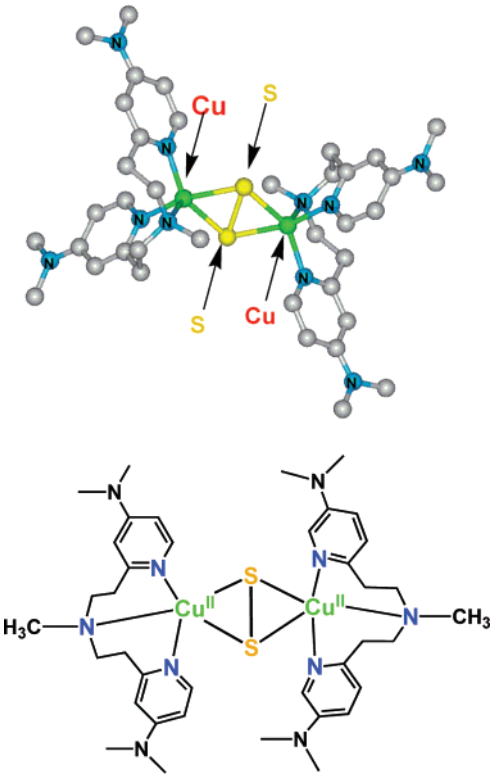

(22) Dooley, D. M.; Chan, J. M. Copper Enzymes in Denitrification. In *Encyclopedia of Inorganic Chemistry*, 2nd ed.; King, R. B., Ed.; Wiley & Sons: Chichester, 2005; Vol. II, pp 1081−1091.
(23) Hammerl, A.; Klapötke, T. M. Nitrogen: Inorganic Chemistry. In *Encyclopedia of Inorganic Chemistry*, 2nd ed.; King, R. B., Ed.; Wiley & Sons: Chichester, 2005; Vol. VI, pp 3531−3599.
(24) Leont'ev, A. V.; Fomicheva, O. A.; Proskurnina, M. V.; Zefirov, N. S. *Russ. Chem. Rev.* **2001**, *70*, 91−104.
(25) Chan, J. M.; Bollinger, J. A.; Grewell, C. L.; Dooley, D. M. *J. Am. Chem. Soc.* **2004**, *126*, 3030−3031.
(26) Rasmussen, T.; Brittain, T.; Berks, B. C.; Watmough, N. J.; Thomson, A. J. *Dalton Trans.* **2005**, 3501−3506.
(27) Lam, W. H.; Cheng, E. C. C.; Yam, V. W. W. *Inorg. Chem.* **2006**, *45*, 9434−9441.
(28) Yang, R. N.; Sun, Y. A.; Hou, Y. M.; Hu, X. Y.; Jin, D. M. *Inorg. Chim. Acta* **2000**, *304*, 1−6.

diode array spectrophotometer equipped with a two-window quartz H. S. Martin Dewar filled with cold MeOH (25 to −85 °C) maintained and controlled by a Neslab VLT-95 low-temperature circulator was attached to the HP spectrophotometer. Spectrophotometer cells used were made by Quark Glass with column and pressure/vacuum side stopcock and 2-mm path length. For the low-temperature measurements with the Cary-50 Bio spectrophotometer, a pentane/$N_2(l)$ bath (−124 °C) was used, and the steady temperature was monitored with the type T thermocouple thermometer (model 650, Omega Engineering). Dioxygen was dried by passing through a short column of supported P_4O_{10} (Aquasorb, Mallinckrodt) and was bubbled into reaction solutions via an 18-gauge, 24-in.-long stainless steel syringe needle. IR spectra were collected using a Mattson Instruments Galaxy series FT-IR (model 4030) that was controlled by the PC program WinFIRST. The copper(I) complex used for low-temperature UV−vis and all reactivity studies reported here are the $B(C_6F_5)_4^-$ salt complexes unless otherwise stated. ESI mass spectra were acquired using a Finnigan LCQDeca ion-trap mass spectrometer equipped with an electrospray ionization source (Thermo Finnigan). Samples were dissolved in CH_3OH and introduced into the instrument at a rate of 10 μL/min using a syringe pump via a silica capillary line. The heated capillary temperature was 250 °C, and the spray voltage was 5 kV. X-ray diffraction was performed at the X-ray diffraction facility at the Johns Hopkins University. The X-ray intensity data were measured on an Oxford Diffraction Xcalibur3 system equipped with a graphite monochromator and an Enhance (Mo) X-ray Source ($\lambda = 0.71073$ Å) operated at 2 kW power (50 kV, 40 mA) and a CCD detector. The frames were integrated with the Oxford Diffraction *CrysAlisRED* software package.

Synthesis of TMPA′. To 6ClTMPA[29] (1.2 g, 3.54 mmol) dissolved in 50 mL of methanol placed in a 250 mL round-bottom flask were added NaOMe (0.288 g, 5.33 mmol) (Aldrich) and KI (0.295 g, 1.77 mmol) dissolved in a few drops of water. The reaction mixture was refluxed under argon at 70 °C overnight. The cooled (to room temperature, RT) mixture was concentrated under reduced pressure to give a reddish brown oily mixture that was dissolved in 100 mL of dichloromethane and filtered. Upon being concentrated under reduced pressure, the mixture was chromatographed on alumina (Activated Alumina, chromatographic grade, 80−200 mesh) using 2% (progressively brought to 5%) methanol in dichloromethane as eluant. The product fraction was collected, and the solvent was removed under reduced pressure to afford the reddish-yellow solid **TMPA′** (0.77 g, 65% yield) ($R_f = 0.43$, alumina, 3% methanol, 97% dichloromethane). ^{1}H NMR ($CDCl_3$): δ 3.46 (s, 3H, CH_3), 3.87 (s, 6H, $3CH_2$), 4.53 (s, 2H, CH_2O), 7.12 (t, 2H; 6.0 Hz), 7.32 (d, 1H; 8.4 Hz), 7.53−7.77 (m, 6H), 8.52 (d, 2H; 4.8 Hz). Anal. Calcd for **TMPA′**: C, 71.83; H, 6.63; N, 16.75. Found: C, 71.41; H, 6.70; N, 16.71. ESI-MS (357, M + Na).

Synthesis of Copper(I) Complex, [(TMPA′)Cu^I]$^+$ (1). TMPA′ (0.169 g, 0.506 mmol) and $[Cu^I(CH_3CN)_4]B(C_6F_5)_4$[30] (0.459 g, 0.506 mmol) were placed in a 100 mL Schlenk flask under argon. Dioxygen-free THF (5 mL) was added under argon to the mixture of solids to form a yellow solution. The resulting solution was stirred under argon for 30 min. Dioxygen-free pentane (60 mL) was then added to the solution to precipitate a yellow solid. The supernatant was decanted, and the solid was recrystalized three times from THF/pentane. The solid obtained was washed with pentane and dried under vacuum (2 h), giving 0.402 g of yellow powder (69% yield). X-ray quality crystals of this compound [(**TMPA′**)Cu^I]$B(C_6F_5)_4$ (**1**) were obtained (Figure 1) after precipitation prompted by pentane, from the ether solution of the yellow complex. Anal. Calcd for **1**-$B(C_6F_5)_4\cdot(H_2O)\cdot(THF)_{0.37}$; $C_{45.5}H_{27}BCuF_{20}N_4O_{2.4}$: C, 48.70; H, 2.43; N, 4.99. Found: C, 48.36; H, 2.49; N, 4.97. ^{1}H NMR (DMSO): δ 1.76 (m, 1.5H, THF), 3.33 (2H, H_2O), 3.47 (s, 3H, CH_3), 3.60 (m, 1.5H, THF), 4.19 (6H, $3CH_2$), 4.75 (s, 2H, CH_2O), 7.1−7.5 (br), 7.6−7.9 (br), 8.66 (2H).

Reaction of [(TMPA)Cu^I(CH$_3$CN)]$^+$ (3) with Elemental Sulfur. [(**TMPA**)Cu^I(CH_3CN)]$^+$ (**3**)[31] (0.010 g, 0.009 mmol) was dissolved in 8 mL of THF in a glovebox and taken in a UV−vis cuvette. Solid elemental sulfur (0.0500 g) was taken in a 25 mL Schlenk flask in a glovebox and was dissolved in 10 mL of THF upon being stirred. This sulfur solution was cooled at −80 °C in an acetone/dry ice bath. The cuvette was cooled to −80 °C, and an initial spectrum was recorded. THF solution (45 μL, 0.007 mmol) of elemental sulfur was added via the microliter syringe to the copper(I) solution **3**. Argon was purged for 10 s. An immediate color change occurred from yellow to purple, and the resulting solution was kept at −80 °C for 5 min (Figure 3A, blue spectrum). Another 45 μL (0.007 mmol) of the THF solution of elemental sulfur was added via the microliter syringe, argon was purged with a long needle, and the following spectrum was recorded (Figure 3A, red spectrum). The green spectrum of Figure 3A was recorded after addition of another 90 μL (0.014 mmol) of sulfur solution and argon purging. No spectral change was observed upon further addition of sulfur solution.

Generation of Disulfido−Dicopper (II) Complex, [{(TMPA′)-Cu^{II}}$_2$(μ-1,2-S_2^{2-})]$^{2+}$ (2). Complex **1** (0.0214 g, 0.018 mmol) was dissolved in 1.8 mL of THF under argon in a 10 mL Schlenk flask. Solid elemental sulfur (0.0059 g) was dissolved in 1 mL of THF upon being stirred in a 5 mL Schlenk flask under argon. This sulfur solution was cooled at −80 °C in an acetone/dry ice bath. The glass stoppers from both flasks were interchanged with rubber septa. From the stock solution of sulfur soutlion, 110 μL of solution (0.020 mmol) was added to the copper(I) solution. Purging argon for 10 s caused thorough mixing of sulfur solution with the copper(I) solution, and the resulting solution was kept at −80 °C for 5 min. An immediate color change occurred from yellow to purple [{(**TMPA′**)Cu^{II}}$_2$(μ-1,2-S_2^{2-})]$^{2+}$ (**2**) {$\lambda_{max} = 540$ nm}. The product disulfide complex **2** is only stable at −80 °C; upon warming to room temperature it became colorless, whereas cooling again to −80 °C (under Ar) resulted in reformation of purple complex **2**. As followed by UV−vis spectroscopy (Figure 3B), formation of purple species **2** required ∼60 s under the conditions described.

Synthesis of [{(TMPA′)Cu^{II}}$_2$(μ-1,2-$^{34}S_2^{2-}$)](B(C_6F_5)$_4$)$_2$. [(**TMPA′**)-Cu^I]$B(C_6F_5)_4$ (**1**) (0.0973 g, 0.085 mmol) was dissolved in 4 mL of THF under argon in a 10 mL Schlenk flask. Solid, isotopically labeled, elemental sulfur (0.0361 g; $^{34}S_8$, 90%, Icon Services, Inc.) was separately dissolved in 1 mL of THF solution by being stirred in a 5 mL Schlenk flask under argon. This sulfur solution was cooled at −80 °C in an acetone/dry ice bath. The glass stoppers from both flasks were interchanged with rubber septa under argon atmosphere. From the stock copper(I) solution, 500 μL of solution (thus 0.0122 g, 0.010 mmol of **1**) was taken into a Wilmad tube (WG-5M-ECONOMY). Ten microliters of 34-labeled sulfur solution (0.010 mmol) was then transferred to the Wilmad tube by microliter syringe. With a long needle that can reach the bottom of the Wilmad tube, we purged the argon for 10 s to ensure thorough mixing; the resulting solution was kept at −80 °C for 5 min while the solution color changed from yellow to purple. After the solution was frozen using liquid N_2, it was sent in a "dry shipper" to Stanford University for resonance Raman spectroscopic analysis.

Low-Temperature Reversible Sulfur Binding to [(TMPA′)Cu^I]$^+$ (1). Under argon atmosphere, [(**TMPA′**)Cu^I]$^+$ (**1**) (0.0214 g, 0.018 mmol) was dissolved in 1.8 mL of THF under argon in a UV−vis cuvette and was cooled to −80 °C. With a microliter syringe, 110 μL of sulfur solution (0.020 mmol) (prepared by dissolving 0.0059 g sulfur in 1 mL of THF) was added to the copper(I) solution. During this process, the sulfur solution added to the copper(I) solution was placed on top of the solution phase in the UV−vis cuvette. With a long needle,

(29) Lucchese, B.; Humphreys, K. J.; Lee, D.-H.; Incarvito, C. D.; Sommer, R. D.; Rheingold, A. L.; Karlin, K. D. *Inorg. Chem.* **2004**, *43*, 5987−5998.
(30) Liang, H. C.; Kim, E.; Incarvito, C. D.; Rheingold, A. L.; Karlin, K. D. *Inorg. Chem.* **2002**, *41*, 2209−2212.
(31) Tyeklár, Z.; Jacobson, R. R.; Wei, N.; Murthy, N. N.; Zubieta, J.; Karlin, K. D. *J. Am. Chem. Soc.* **1993**, *115*, 2677−2689.

we purged argon for 10 s to ensure thorough mixing of sulfur solution with the copper(I) solution. The resulting solution in cuvette was kept at −80 °C, the color changed from yellow to purple, and complex **2** and the spectrum were recorded. Warming to RT caused the reformation of initial spectrum of copper(I) species of **1**. Cooling to −80 °C regenerated **2** completely. This cycle can be performed several times under inert atmosphere (10 cycles were performed) without any decrease in absorption intensity (Figure S4, Supporting Information).

Reaction of [{(TMPA′)Cu^{II}}$_2$(μ-1,2-S_2^{2-})]$^{2+}$ (2) with CO. A deoxygenated 3.1 mL THF solution of **2** (0.0120 g, 0.005 mmol) at −80 °C reacted with CO in a reversible fashion; bubbling with CO gas caused an immediate bleaching of the purple color as seen by the loss of all absorption features (Figure 6). This colorless solution was independently determined as the copper(I) carbonyl adduct of **TMPA′**, [(**TMPA′**)Cu^{I}(CO)]$^{+}$ (**8**), as defined by its FTIR spectrum, which had a distinct CO stretch at 2094 cm^{-1} (Figure S5, Supporting Information). Bubbling this colorless solution with argon for 5 min at −80 °C led to reformation of the solution's purple color, which was concomitant with a growth in the absorption features related to **2**. This suggested that, during CO reaction with **2**, elemental sulfur formation occurred, because no additional sulfur from outside was added. The colorless solutions formed by CO bubbling of the purple solution of **2** described above led to the isolation of **8** (0.0089 g, 75% yield) following precipitation with 25 mL of pentane and recrystallization from CO-saturated solutions of THF/pentane. Anal. Calcd for [(**TMPA′**)Cu^{I}(CO)]B(C_6F_5)$_4$·H_2O; $C_{45}H_{24}BCuF_{20}N_4O_3$: C, 48.13; H, 2.15; N, 4.99; Found: C, 47.86; H, 1.99; N, 5.37. ^{1}H NMR (DMSO): δ 3.33 (2H, H_2O), 3.47 (s, 3H, CH_3), 4.20 (6H, 3CH_2), 4.76 (s, 2H, CH_2O), 7.1−7.5 (br), 7.7−7.9 (br), 8.7 (d, 2H).

Reaction of [{(TMPA′)Cu^{II}}$_2$(μ-1,2-S_2^{2-})]$^{2+}$ (2) with TMPA. Complex **1** (0.0057 g, 0.005 mmol) was dissolved in 3.2 mL of THF under argon in a UV−vis cuvette. This cuvette was cooled to −80 °C, and an initial spectrum was recorded. Solid elemental sulfur (0.0084 g) was dissolved in 5 mL of THF upon being stirred in a 10 mL Schlenk flask under argon. This sulfur solution was cooled at −80 °C in an acetone/dry ice bath. Sulfur solution (100 μL, 0.005 mmol) was added to the copper(I) solution. With a long needle, argon was purged for 10 s, and the resulting solution in cuvette was kept at −80 °C. The color change occurred from yellow to purple complex **2**. The spectrum of **2** was recorded. Under argon atmosphere, 0.0316 g of **TMPA** was dissolved in 1 mL of THF. Anaerobically, 50 μL of THF solution of **TMPA** (0.005 mmol) was added to this purple solution, and immediate color change occurred from purple to deep blue. Another 50 μL of THF solution of **TMPA** was added, and the spectrum was recorded. Further addition of sulfur solution was performed, and no change in spectrum was observed. Thus, the addition of **TMPA** caused generation of species with absorption features at 568, 649, and 847 nm, which was identical to that observed for solutions from [(**TMPA**)-Cu^{I}(CH_3CN)]$^{+}$ (**3**)/S_8 reactivity (Figure 3A).

Reaction of [{(TMPA′)Cu^{II}}$_2$(μ-1,2-S_2^{2-})](B(C_6F_5)$_4$)$_2$ with O_2. A 3.9 mL 2-methyltetrahydrofuran (MeTHF) solution of **1** (0.0057 g, 0.005 mmol) was taken in a UV−vis cuvette under argon and 100 μL of a MeTHF solution, which was 0.005 mM (prepared by adding 0.0167 g of S_8 in 10 mL of MeTHF). The cuvette was cooled to −124 °C, and an initial spectrum of **2** was recorded {λ_{max} = 540 nm (ϵ, 4600 M^{-1} cm^{-1})}. Dry dioxygen was bubbled for 30 s through the solution using a long syringe needle, and the spectrum recorded is shown in Figure 7. Additional bubbling did not change the spectrum further. As described below, the product forms appeared to be [{(**TMPA′**)Cu^{II}}$_2$(O_2)]$^{2+}$ (**9**), a μ-1,2-peroxodicopper(II) complex {λ_{max} = 540 nm (ϵ, 9550 M^{-1}cm^{-1}) and 610 nm, sh (ϵ, 6500 M^{-1} cm^{-1})}.

Reaction of [(TMPA′)Cu^{I}]$^{+}$ (1) with O_2. A 3.8 mL THF solution of **1** (0.0049 g, 0.004 mmol) was taken in a UV−vis cuvette under argon. The cuvette was cooled to −80 °C, and an initial spectrum was recorded. Dry dioxygen was bubbled for 30 s through the solution using a long syringe needle, and the spectrum recorded is shown in Figure S6, Supporting Information. Additional bubbling did not change the spectrum further. The purple product forms appeared to be [{(**TMPA′**)-Cu^{II}}$_2$(O_2)]$^{2+}$ (**9**), a μ-1,2-peroxodicopper(II) complex. Upon warming to RT, the purple species **9** decomposed to a green species that cannot be used to reform **9**. Thus, with respect to temperature, the reactivity of **1**/O_2 is irreversible.

Reaction of [{(TMPA′)Cu^{II}}$_2$(μ-1,2-S_2^{2-})](B(C_6F_5)$_4$)$_2$ with PPh_3. Compound **1** (0.0485 g, 0.042 mmol) was dissolved in 4 mL of THF under argon in a 10 mL Schlenk flask, elemental sulfur (0.0014 g, 0.043 mmol) was added, and the solution was stirred under argon. After being cooled to −80 °C using an acetone/dry ice bath, 100 μL of a THF solution prepared by dissolving PPh_3 (0.220 g, 0.839 mmol) in 1 mL of THF was added anaerobically and the reaction was kept at −80 °C for 8 h. A quantity of 200 μL of solution was taken from the resulting solution for quantitative analysis by ^{31}P NMR at room temperature with P(Mes)$_3$ as reference: (400 MHz); δ 43.37 (S═PPh_3), 3.41 ([(**TMPA′**)Cu^{I}(PPh_3)](B(C_6F_5)$_4$); (**11**), −35.91 (P(Mes)$_3$) ppm. On the basis of integration, the ratio of S═PPh_3/(**11**) (∼1:0.9) showed that the reaction was 90% complete. The copper complex was then precipitated from product solution by addition of 50 mL of pentane. Analysis of the supernatant by GC and GC−MS (see below for conditions) confirmed the formation of S═PPh_3 (0.012 g, 95% yield); authentic commercial S═PPh_3 was also used for comparison. The copper product, [(**TMPA′**)Cu^{I}(PPh_3)]B(C_6F_5)$_4$; (**11**)-B(C_6F_5)$_4$ (0.0478 g, 85% yield), was isolated by redissolving the precipitate obtained (above) in THF, adding pentane again and recrystallizing from THF/pentane. The precipitate was dried in vacuo and analyzed by ^{31}P NMR in THF with P(Mes)$_3$ as reference: (400 MHz); δ 3.40 (**11**), −35.91 (P(Mes)$_3$) ppm. The ^{1}H NMR (DMSO, RT): δ 3.37 (s, 3H, CH_3), 4.10 (6H, 3CH_2), 4.42 (s, 2H, CH_2O), 7.1−7.5 (m), 7.6−7.9 (m), 8.6 (d, 2H). Anal. Calcd for **11**; $C_{62}H_{37}BCuF_{20}N_4OP$: C, 55.60; H, 2.78; N, 4.18. Found: C, 55.30; H, 2.78; N, 4.21.

In a similar approach, compound **1** (0.162 g, 0.14 mmol) was dissolved in 3 mL of THF under argon in a 10 mL Schlenk flask, elemental sulfur (0.0045 g, 0.14 mmol) was added, and the solution was stirred under argon. After being cooled to −80 °C using an acetone/dry ice bath, 100 μL of a THF solution (0.036 g, 0.14 mmol) prepared by dissolving PPh_3 (0.36 g) in 1 mL of THF was added anaerobically, and the reaction was kept at −80 °C for 8 h. ^{31}P NMR was recorded at room temperature with P(Mes)$_3$ as reference: (400 MHz); δ 43.37-(S═PPh_3), 3.41 ([(**TMPA′**)Cu^{I}(PPh_3)](B(C_6F_5)$_4$); (**11**), −35.91(P(Mes)$_3$) ppm which shows near 1:0.85 integration of S═PPh_3 and **11**.

Reaction of [{(TMPA′)Cu^{II}}$_2$(μ-1,2-S_2^{2-})](B(C_6F_5)$_4$)$_2$ with ArNC. Compound **1** (0.0501 g, 0.043 mmol) was dissolved in 3.5 mL of THF under argon in a 10 mL Schlenk flask, elemental sulfur (0.0014 g, 0.043 mmol) was added, and the solution was stirred under argon. After being cooled to −80 °C using an acetone/dry ice bath, 100 μL of a THF solution prepared by dissolving 2,6-dimethylphenyl isocyanide (ArNC) (0.114 g, 0.870 mmol) in 1 mL of THF was added anaerobically, and the reaction was kept cold at −80 °C for 1 h. The copper complex was then precipitated from product solution by addition of 40 mL of pentane. Analysis of the supernatant by GC and GC−MS (see below for conditions) confirmed the formation of 2,6-dimethylphenyl isothiocyanate (ArNCS) in ∼85% yield; authentic commercial ArNCS was also used for comparison. The copper product, [(**TMPA′**)Cu^{I}(CNAr)]$^{+}$ (**12**), was isolated by redissolving the precipitate obtained (above) in THF and recrystallizing from THF/pentane. The intraligand cyanate stretching ν(N≡C) in **12** (in acetone) occurred at 2140 cm^{-1}. The precipitate was dried under vacuum and analyzed by ^{1}H NMR ($CDCl_3$): δ 1.6 (2.8H, H_2O), 2.6 (s, CH_3, ArNC), 3.4 (s, 3H, CH_3), 4.1 (s, 4H, 2CH_2), 4.2 (s, 2H, CH_2), 4.7 (s, 2H, CH_2O), 7.1−7.4 (m), 7.6−7.8 (m), 8.6 (d, 2H). Anal. Calcd. For [(**TMPA′**)Cu^{I}(CNAr)]B(C_6F_5)$_4$·(H_2O)$_{1.4}$; $C_{53}H_{33.8}$-$BCuF_{20}N_5O_{2.4}$: C, 51.61; H, 2.76; N, 5.68. Found: C, 51.54; H, 2.50; N, 5.57.

Reaction of [{(TMPA′)Cu^{II}}$_2$(μ-1,2-S_2^{2-})](B(C_6F_5)$_4$)$_2$ (2) with $PhCH_2Br$. Compound **1** (0.0486 g, 0.043 mmol) was dissolved in 4

mL of THF under argon in a 10 mL Schlenk flask, and elemental sulfur (0.0014 g, 0.043 mmol) was added upon strirring. After being cooled to −80 °C using an acetone/dry ice bath, 200 μL of a THF solution prepared by dissolving $PhCH_2Br$ (0.072 g, 0.428 mmol) in 1 mL of THF was added anaerobically; the purple solution turned green over the course of 8 h. The copper complex was then precipitated from the product solution by addition of 50 mL of pentane. Analysis of the supernatant by GC and GC−MS (see below for conditions) confirmed the formation of $PhCH_2SSCH_2Ph$, $PhCH_2SCH_2Ph$, and $PhCH_2SSSCH_2Ph$ in ∼70, ∼10, and ∼15% yield, respectively; authentic commercial $PhCH_2SSCH_2Ph$, $PhCH_2SCH_2Ph$, and $PhCH_2SSSCH_2Ph$ were also used for comparison. The green product, **[**{(**TMPA′**)Cu^{II}(Br)}$_2$](B$(C_6F_5)_4)_2$ (**6**) (0.0349 g, 71% yield), was isolated by redissolving the precipitate obtained (above) in THF, adding pentane again, and recrystallizing from THF/pentane. IR and UV−vis spectra of **6** also matched a sample of independently synthesized **[**{(**TMPA′**)Cu^{II}(Br)}$_2$](B$(C_6F_5)_4)_2$ (**6**) (see below) (Figures S2 and S3, Supporting Information). Anal. Calcd for **6**, {$C_{44}H_{22}BBrCuF_{20}N_4O$}$_2$: C, 45.68; H, 1.92; N, 4.84. Found: C, 45.91; H, 2.04; N, 4.93.

Synthesis of [{(**TMPA′**)Cu^{II}(Br)}$_2$](B$(C_6F_5)_4)_2$ (6).** Complex **1** (0.112 g, 0.097 mmol) was dissolved in 5 mL of dioxygen-free THF under an argon atmosphere and added to a 25 mL Schlenk flask. Deoxygenated $CHBr_3$ (0.5 mL) was then added under argon, whereupon the solution ceased to look transparent, and its color instantly turned to green. After 1 h, 40 mL of pentane was added to precipitate the copper complex. The precipitate was redissolved in THF and again precipitated using pentane. The green crystalline material was further purified by recrystallization from $CHBr_3$/pentane. After being vacuum-dried, the green crystals weighed 0.078 g (yield, 65%). Confirmation of the formation and identity of this complex came from X-ray crystallography. IR and UV−vis spectra of **[**{(**TMPA′**)Cu^{II}(Br)}$_2$](B$(C_6F_5)_4)_2$ (**6**) was recorded and compared with the copper product generated from the reaction of [{(**TMPA′**)Cu^{II}}$_2$(μ-1,2-S_2^{2-})](B$(C_6F_5)_4)_2$ (**2**) and $PhCH_2Br$ (Figures S2 and S3, Supporting Information).

Synthesis of [{(**TMPA′**)Cu^{II}(Cl)}$_2$](B$(C_6F_5)_4)_2$ (7).** Complex **1** (0.150 g, 0.130mmol) was dissolved in 5 mL of dioxygen-free THF under an argon atmosphere and added to a 25 mL Schlenk flask. The resulting yellow solution was stirred at room temperature under argon atmosphere. Deoxygenated $CHCl_3$ (0.5 mL) was then added under argon, whereupon the solution ceased to look transparent, and its color instantly turned to green. After 1 h, 40 mL of pentane was added to precipitate the copper complex. The precipitate was redissolved in THF and again precipitated using pentane. X-ray quality crystals of this compound **[**{(**TMPA′**)Cu^{II}(Cl)}$_2$](B$(C_6F_5)_4)_2$ (**7**) were obtained (Figure S1 and Table S2, Supporting Information) after precipitation prompted by pentane from the reaction solution. After being vacuum-dried, the green crystals weighed 0.104 g (70%). Anal. Calcd for {$C_{44}H_{22}$-$BClCuF_{20}N_4O{\cdot}H_2O$}$_2$: C, 46.75; H, 2.14; N, 4.96. Found: 46.83; H, 2.39; N, 4.91. Infrared (Nujol Mull): 3480 cm^{-1} (w, br) (indicating the presence of the formulated water).

Reaction of [{(**TMPA**)Cu^{II}}$_2$(μ-1,2-S_2^{2-})](B$(C_6F_5)_4)_2$ (4) with $PhCH_2Br$.** [(**TMPA**)$Cu^{I}(CH_3CN)]^+$ (**3**) (0.050 g, 0.046 mmol) was dissolved in 4 mL of THF in a glovebox, taken in a 10 mL Schlenk flask, and cooled to −80 °C. Solid elemental sulfur (0.044 g) was taken in a 10 mL Schlenk flask in a glovebox and was dissolved in 2 mL of THF upon being stirred. This sulfur solution was cooled at −80 °C in an acetone/dry ice bath. THF solution (200 μL, 0.1375 mmol) of elemental sulfur was added via the microliter syringe to the copper(I) solution of **3**. With a long needle, we purged argon for 10 s to ensure the thorough mixing of sulfur solution with the copper(I) solution. An immediate color change occurred from yellow to deep blue, and the resulting solution was kept at −80 °C for 5 min. THF solution (200 μL) prepared by dissolving $PhCH_2Br$ (0.0156 g, 0.093 mmol) was added anaerobically, and the resulting solution was kept cold for 8 h. The copper complex was then precipitated from the product solution by addition of 50 mL of pentane. Analysis of the supernatant by GC and GC−MS (see below for conditions) confirmed the formation of $PhCH_2SSCH_2Ph$, $PhCH_2SCH_2Ph$, and $PhCH_2SSSCH_2Ph$ in ∼12, ∼5, and ∼75% yield, respectively; authentic commercial $PhCH_2SSCH_2Ph$, $PhCH_2SCH_2Ph$, and $PhCH_2SSSCH_2Ph$ were also used for comparison.

Scheme 1

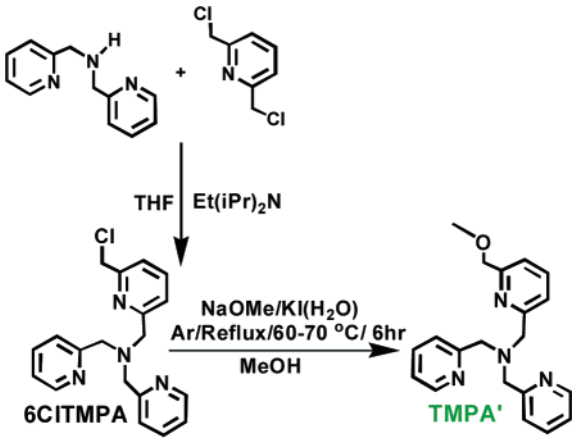

GC and GC−MS Analysis of the Reactants and Products from $PhCH_2Br$, PPh_3, and ArNC Reaction with 2. All GC−MS experiments were carried out and recorded using a Shimadzu GC-17A/GCMS0QP5050 gas chromatograph/mass spectrometer. All GC experiments were carried out and recorded using a Hewlett-Packard 5890 Series II gas chromatograph.

The GC conditions for the analysis of the products were:

Injector port temperature, 250 °C; detector temperature, 250 °C; column temperature, initial temperature, 120 °C; initial time, 2 min; final temperature, 250 °C; final time, 15 min; gradient rate, 30 °C/min; flow rate, 51 mL/min.

The GC−MS conditions for the product analysis were:

Injector port temperature, 220 °C; detector temperature, 280 °C; column temperature, initial temperature, 120 °C; initial time, 2 min; final temperature, 250 °C; final time, 15 min; gradient rate, 10 °C/min; flow rate, 16 mL/min; ionization voltage, 1.5 kV.

Resonance Raman Experimental Procedure. Resonance Raman spectroscopy measurements were undertaken on a Princeton Instruments ST-135 back-illuminated CCD detector on a Spex 1877 CP triple monochromator with 1200, 1800, and 2400 grooves/mm holographic spectrograph gratings. Excitation was provided by a Coherent I90C-K Kr+ ion laser (λ_{ex} = 530). The spectral resolution was <2 cm^{-1}. Sample concentrations were approximately 5.5 mM in Cu_2S_2. Samples were run at 77 K in a liquid N_2 finger Dewar (Wilmad).

Results and Discussion

Ligand Synthesis. The synthesis of the **TMPA′** is straightforward, gram quantities of the ligand could be readily obtained (Scheme 1), and it was characterized by elemental analysis, ^{1}H NMR spectroscopy, and ESI-MS (see Experimental Section).

X-ray Structure of [(TMPA′)Cu^{I}]B$(C_6F_5)_4$ (1-B$(C_6F_5)_4$). An ORTEP diagram of the cationic portion of **1**-B$(C_6F_5)_4$ is presented in Figure 1. The structure is five-coordinate, with ligation to the three pyridyl and single aliphatic nitrogen atoms of the ligand, accompanied by a weaker interaction of the cuprous ion with the ether oxygen atom (O1), Cu−O = 2.545 (3) Å. Selected bond distances and angles are provided in the Figure 1 caption, and a full listing is given in Supporting Information (Table S1). The geometry about the copper atom is trigonal bipyramidal with the amine nitrogen N2 occupying the axial position and the pyridyl nitrogens (N1, N3, N4) in the trigonal plane. The Cu(I) ion is displaced 0.315 (8) Å out of the N1−N3−N4 plane, in fact toward O1. The equatorial values

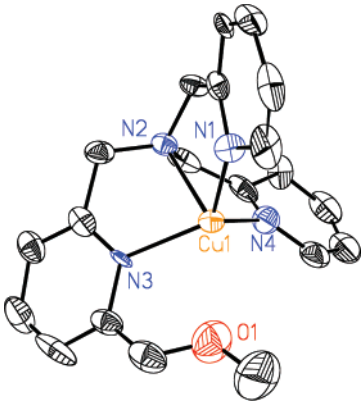

Figure 1. X-ray structure of the copper(I) complex [(**TMPA′**)Cu^{I}]$B(C_6F_5)_4$ (**1**). The thermal ellipsoids are at the 50% probability level, and the hydrogen atoms and the minor disorder component (see Supporting Information) are omitted for clarity.

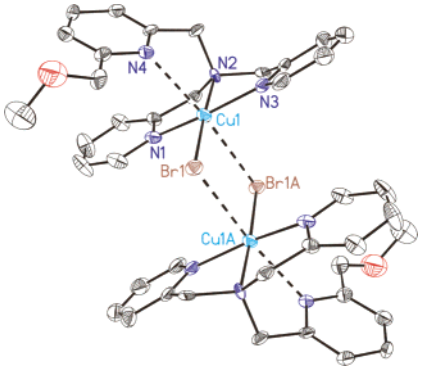

Figure 2. ORTEP diagram of [{(**TMPA′**)Cu^{II}(Br)}$_2$]$(B(C_6F_5)_4)_2$ (**6**): Cu1−Br1 = 2.3859 (12) Å; Cu1−Br1A = 3.0033 (1) Å; Cu1−N4 = 2.508 (6) Å. Also, see text and Supporting Information.

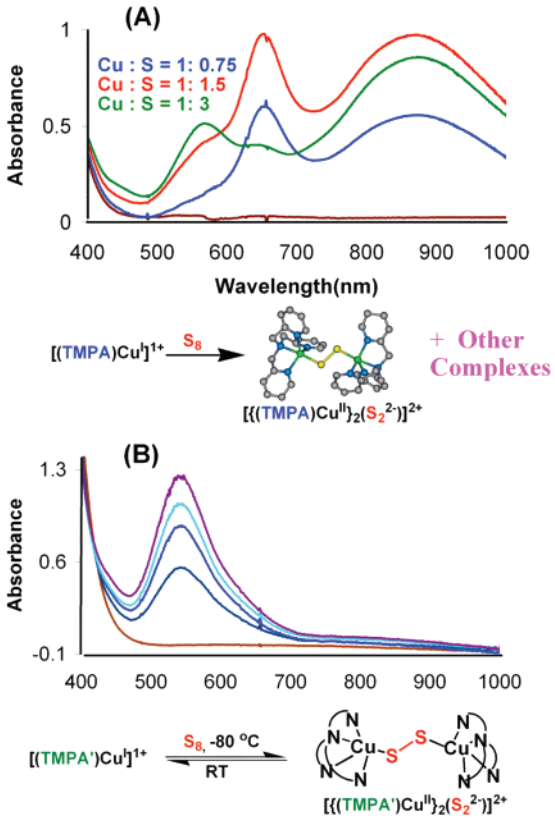

Figure 3. UV−vis spectra at −80 °C in THF solvent, illustrating that (A) mixtures of complexes form in reaction of [(**TMPA**)$Cu^{I}(CH_3CN)]^+$ (**3**)/*x*·S (*x* = 0.75 to 3; S in the form of S_8) but (B) only the end-on disulfide complex [{(**TMPA′**)Cu^{II}}$_2$(μ-1,2-S_2^{2-})]$^{2+}$ (**2**) is generated from [(**TMPA′**)-$Cu^{I}]^+$ (**1**)/*y*·S (*y* = 0.5 to 1.5). Full formation of **2** occurs within 60 s for *y* > 1. See text.

($Cu-N_{pyridine}$) are in the range 1.984(2)−2.051(2) Å and shorter than the $Cu-N_{amine}$ bond length of Cu1−N2 = 2.238 (2) Å. X-ray crystal structures for a number of copper(I) complexes with pyridylalkylamine tripodal tetradentate ligands have been described,[32−34] sharing this structural motif, being distorted from tetrahedral toward trigonal bipyramidal. A difference in the present structure is that the Cu(I) ion resides on the opposite side of the pyridyl basal plane, undoubtedly because of the interaction with the ether oxygen O1.

[(TMPA′)Cu^{I}]$B(C_6F_5)_4$ (1) and Reactions with Halogenated Compounds. The copper(I) complex with **TMPA′** was prepared in a typical manner using $[Cu^{I}(CH_3CN)_4]B(C_6F_5)_4$[30] as the copper source (see Experimental Section). As we have seen many times previously[29,31,35,36] and known in other cases,[37−39] copper(I) complexes such as **1** are reactive toward organohalides, resulting in the production of halide copper(II) products. Here, we utilized this organohalide reaction chemistry (eq 1) to generate a dimeric bromide complex [{(**TMPA′**)Cu^{II}-(Br)}$_2$]$(B(C_6F_5)_4)_2$ (**6**), which was needed as a standard to identify a separate product formed in another reaction of interest (see below). Exposure of **1** to $CHBr_3$ in THF solvent led to an immediate reaction (according to eq 1), and **6** was isolated in high yield; its X-ray structure is given and described below. We also generated the chloride analogue [{(**TMPA′**)Cu^{II}(Cl)}$_2$]-$(B(C_6F_5)_4)_2$ (**7**) by reaction of **1** with $CHCl_3$ in THF and obtained its structure, which is deposited in the Supporting Information.

$$[(\mathrm{TMPA'})Cu^{I}]^+ + R-X \rightarrow [(\mathbf{TMPA'})Cu^{II}(X)]^+ + R\cdot \rightarrow\rightarrow \quad (1)$$

X-ray Structure of [{(TMPA′)Cu^{II}(Br)}$_2$]$(B(C_6F_5)_4)_2$ (6). The structure of **6** is dimeric, where bromide bridging occurs via equatorial/axial bonding (Figure 2). Each copper ion is hexacoordinate where the **TMPA′** donors (N1, N2, N3, and Br1) comprise the equatorial plane and the axial positions are occupied by a more weakly coordinated pyridyl nitrogen N4 (Cu−N4 = 2.508 (1) Å) and very elongated Br1A (Cu1−Br1A = 3.0033 (1)). This dimerized structure has previously been observed for a copper(II) complex with **TMPA** and a fluoride ligand.[40] As mentioned, the Cu−N4 bond distance is elongated,

(32) Schatz, M.; Becker, M.; Thaler, F.; Hampel, F.; Schindler, S.; Jacobson, R. R.; Tyeklár, Z.; Murthy, N. N.; Ghosh, P.; Chen, Q.; Zubieta, J.; Karlin, K. D. *Inorg. Chem.* **2001**, *40*, 2312−2322.
(33) Zubieta, J.; Karlin, K. D.; Hayes, J. C. Structural Systematics of Cu(I) and Cu(II) Derivatives of Tripodal Ligands. In *Copper Coordination Chemistry: Biochemical and Inorganic Perspectives*; Karlin, K. D., Zubieta, J., Eds.; Adenine Press: Albany, NY, 1983; pp 97−108.
(34) Karlin, K. D.; Hayes, J. C.; Hutchinson, J. P.; Hyde, J. R.; Zubieta, J. *Inorg. Chim. Acta* **1982**, *64*, L219−L220.
(35) Jacobson, R. R.; Tyeklár, Z.; Karlin, K. D. *Inorg. Chim. Acta* **1991**, *181*, 111−118.
(36) Wei, N.; Murthy, N. N.; Chen, Q.; Zubieta, J.; Karlin, K. D. *Inorg. Chem.* **1994**, *33*, 1953−1965.
(37) Osako, T.; Karlin, K. D.; Itoh, S. *Inorg. Chem.* **2005**, *44*, 410−415.
(38) Osako, T.; Ueno, Y.; Tachi, Y.; Itoh, S. *Inorg. Chem.* **2003**, *42*, 8087−8097.
(39) Komiyama, K.; Furutachi, H.; Nagatomo, S.; Hashimoto, A.; Hayashi, H.; Fujinami, S.; Suzuki, M.; Kitagawa, T. *Bull. Chem. Soc. Jpn.* **2004**, *77*, 59−72.
(40) Jacobson, R. R.; Tyeklár, Z.; Karlin, K. D.; Zubieta, J. *Inorg. Chem.* **1991**, *30*, 2035−2040.

Scheme 2

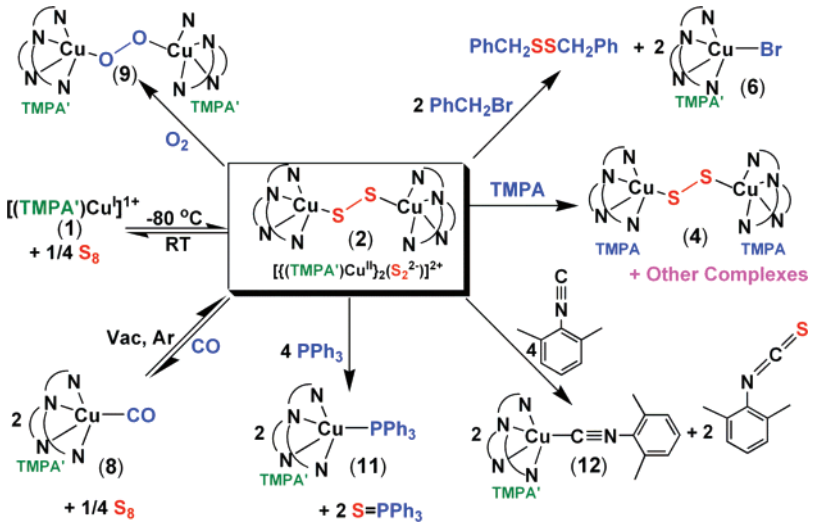

and it is notable this pyridyl plane containing N4 makes a dihedral angle of 45.9 (0.2)° with the best least-squares plane including Cu1, N1, N2, N3, and Br1. This indicates that overlap of the lone pair electrons on N4 and a bonding copper orbital are not ideal. Tables of bond angles and distances for **6**, along with data and comparisons to **7**, are given in the Supporting Information (Table S2).

Titrations of Sulfur with Copper(I) Complex of TMPA. Our first attempt to generate discrete Cu−S complexes by investigating [(**TMPA**)$Cu^{I}(CH_3CN)]^+$ (**3**)/S_8 reactivity led, as mentioned in the Introduction, to the crystallographic characterization of an end-on bound dicopper disulfide complex [{(**TMPA**)Cu^{II}}$_2$(μ-1,2-S_2^{2-})]$^{2+}$ (**4**) (Chart 1, Figure 3A). A UV−vis spectrum of a (**3**)/S_8 derived solution, or even that from crystals of **4** that have been redissolved,[6,11] reveals at least three clear peaks: at 568, 649, and 847 nm (Figure 3A). However, these bands change in their relative intensities, depending on solvent (data not shown, but see ref 11). Furthermore, as shown here (Figure 3A), adding variable amounts of S_8 also leads to different relative intensities. These observations indicate that absorption bands at 568, 649, and 847 nm are different chemical species that are in chemical equilibrium. Previous[11] rR spectra obtained with variable excitation wavelengths and examining associated ^{34}S isotope shifts also confirmed the presence of three species, with the 568 nm absorption associated with the disulfido−dicopper(II) X-ray structure, [{(**TMPA**)Cu^{II}}$_2$(μ-1,2-S_2^{2-})]$^{2+}$ (**4**) (Chart 1). The identity or nature of the other species (λ_{max} = 649 and 847 nm) has yet to be determined. Thus, reactivity studies on solutions of [(**TMPA**)$Cu^{I}(CH_3CN)]^+$ (**3**)/S_8 would not allow any significant conclusions to be drawn, nor would utilization of such solution mixtures be likely useful as synthons for further synthetic manipulation (e.g., reduction toward generation of lower-valent copper−sulfide clusters). This led us to modify the tetradentate ligand system in the hopes of generating a pure end-on bound (μ-1,2-) disulfido−dicopper-(II) analogue complex. We have previously shown that the presence of steric effects coming from 6-pyridyl substituents on the **TMPA** ligand framework affects coordination geometry changes for resulting copper(II) complexes.[29] Namely, a shift from trigonal bipyramidal coordination geometry in [(ligand)$Cu^{II}X]^{+/2+}$ (X = Cl^-, CH_3CN, H_2O, O_2^{2-} (one of the peroxide oxygen atoms)) to square-based pyramidal five-coordinate copper(II) complexes occurs.

Low-Temperature Reaction of Sulfur with [(TMPA′)$Cu^{I}]^+$ (1). We were the first to generate a disulfur−dicopper complex with nitrogenous ligands employing elemental sulfur (S_8) as the sulfur source, via addition to a copper(I) complex.[6] The Fujisawa/Kitajima complex,[5] in fact the first disulfido−dicopper-(II) complex, came about from C−S cleavage of an organothiol leading to a side-on bound disulfido−dicopper(II) complex with tris(pyrazolyl)borate ligands. We have continued to use elemental sulfur,[7] and Tolman and co-workers have since also used S_8[10,12,13] or trimethylsilylsulfide[10] as sulfur sources.

Addition of elemental sulfur (as S_8) to **1** at −80 °C under argon causes an immediate change in color of the solution from yellow to purple; such solutions are very stable, but decreased absorption occurs rapidly even upon slight warming. It should be noted that copper(I) complexes with tetradentate ligands such as **TMPA** and **TMPA′** typically react rapidly and irreversibly with O_2 at room temperature, and normally one needs to decrease the temperature to characterize and study primary or secondary (superoxo-Cu^{II}, binuclear peroxo-Cu^{II}_2, bis-μ-oxo-Cu^{III}_2) Cu^{I}/O_2 adducts.[31,41,42] Titrations of S_8 with the new ligand complex [(**TMPA′**)$Cu^{I}]^+$ (**1**) show that (on the basis of UV−vis criteria and resonance Raman spectroscopy, see below) only one species forms in solution, [{(**TMPA′**)Cu^{II}}$_2$(μ-1,2-S_2^{2-})]$^{2+}$ (**2**), λ_{max} = 540 nm (Figure 3B). (Note: To obtain a true ϵ value for **2**, i.e., under conditions where this species would form to the maximal extent, its generation was carried out at lower temperature in MeTHF at −124 °C; here ϵ_{540} = 4600 M^{-1} cm^{-1}).

Complex Formulation, Purity, and Proposed Structure. We formulate this single solution product of the [(**TMPA′**)-$Cu^{I}]^+$ (**1**)/S_8 reaction as the end-on bound species [{(**TMPA′**)-Cu^{II}}$_2$(μ-1,2-S_2^{2-})]$^{2+}$ (**2**) (λ_{max} = 540 nm) (Scheme 2) because of the similarity of the **TMPA′** and **TMPA** ligands and the known structure of [{(**TMPA**)Cu^{II}}$_2$(μ-1,2-S_2^{2-})]$^{2+}$ (**4**),[6] the similar λ_{max} value of the complex to that of **4** (λ_{max} = 568 nm),

(41) Lee, D.-H.; Wei, N.; Murthy, N. N.; Tyeklár, Z.; Karlin, K. D.; Kaderli, S.; Jung, B.; Zuberbühler, A. D. *J. Am. Chem. Soc.* **1995**, *117*, 12498−12513.
(42) Karlin, K. D.; Lee, D.-H.; Kaderli, S.; Zuberbühler, A. D. *Chem. Commun.* **1997**, 475−476.

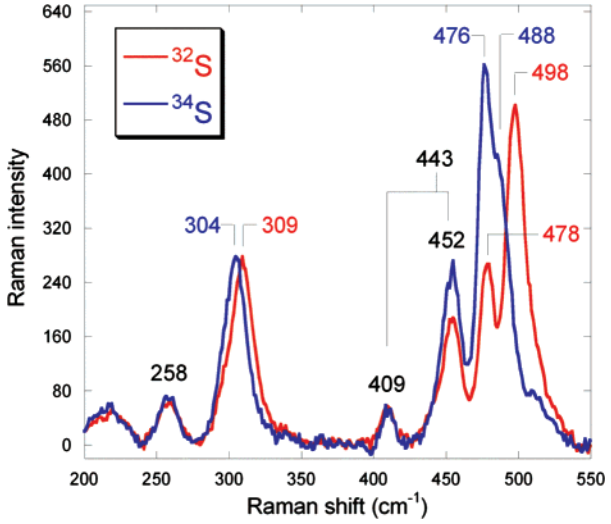

Figure 4. Solvent subtracted resonance Raman spectra of **2**-$(B(C_6F_5)_4)_2$ with naturally abundant sulfur (red) and with isotopically enriched ^{34}S (blue) in THF, with excitation $\lambda = 530$ nm at 77 K.

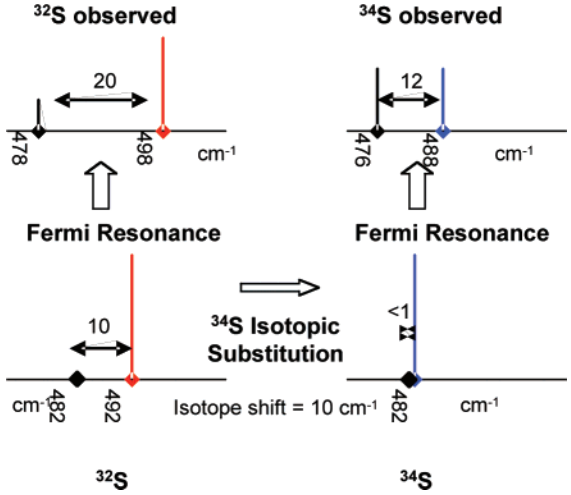

Figure 5. Bottom: Schematic illustration of the pre-interaction Raman peaks for the ^{32}S complex (red) and ^{34}S complex (blue). Top: The observed result of Fermi interaction of a resonance enhanced ν(S−S) mode with a non-enhanced mode of the same symmetry (black).

and the strikingly similar rR spectra of this complex to those of the end-on bound complex **4**,[11] as discussed below. Additionally, the absorption spectrum of this complex is similar to that of the dioxygen adduct with the [(**TMPA**)$Cu^I(CH_3CN)]^+$ (**3**), the end-on μ-1,2-peroxo dicopper(II)−**TMPA** complex, [{(**TMPA**)$Cu^{II}\}_2(\mu$-1,2-$O_2^{2-})]^{2+}$ (**10**) (see Supporting Information, Figure S7). The formulation of **2** as a single species is supported by the solution absorption spectrum of the complex (in sharp contrast to that of **4**, which shows the presence of three distinct chemical species) and is indirectly supported by reactivity studies (Scheme 2), as discussed below.[43] We speculate that small subtle changes in coordination geometry, known to occur with 6-pyridyl substituents on **TMPA** (such as in **TMPA′**),[29] may somehow direct the [(**TMPA′**)$Cu^I]^+$ (**1**)/S_8 chemistry to one product only, namely **2**, and stabilize it to a greater extent than **TMPA** stabilizes **4**.

Resonance Raman Spectroscopy. Resonance Raman spectra of [{(**TMPA′**)$Cu^{II}\}_2(\mu$-1,2-$S_2^{2-})]^{2+}$ (**2**) with ^{32}S and ^{34}S isotopic substitution were collected ($\lambda_{ex} = 530$ nm) and were very similar to previous data collected on **4**.[11,44] On the basis of previous assignment of **4**, the 309 cm^{-1} peak, which shifts to 304 cm^{-1} upon ^{34}S isotopic substitution, is assigned as $\nu(Cu-S)_{sym}$ (Figure 4). The peaks at 498 and 478 cm^{-1} in the ^{32}S Raman spectrum are the result of the Fermi resonance of the ν(S−S) peak with a local non-enhanced mode of the same symmetry. The 488 and 476 cm^{-1} peaks in the ^{34}S Raman spectrum are similarly assigned as a Fermi doublet involving resonance enhancement of the S−S stretch. The unmixed modal energies of the ^{32}S and ^{34}S ν(S−S) stretches were calculated by solving two 2 × 2 matrices with the pre-interaction energies as diagonal elements and the Fermi interaction term as the off-diagonal elements as previously described.[45] From this analysis, the pre-interaction non-enhanced mode is estimated at 482 cm^{-1} for the ^{32}S and ^{34}S spectra and the pre-interaction enhanced ν(S−S) stretches are estimated at 492 and 482 cm^{-1}. Thus, the isotope shift of the ν(S−S) stretch is 10 cm^{-1} upon ^{34}S isotopic substitution (Figure 5). The NCA calculated isotopic shift of this vibration is 11 cm^{-1} in **4**.[11]

On the basis of spectral similarities of this complex with the structurally defined **4**, we can assign **2** as an end-on μ-1,2 disulfido−dicopper(II) complex. As observed for complex **4**, the ν(S−S) value of 492 cm^{-1} for [{(**TMPA′**)$Cu^{II}\}_2(\mu$-1,2-$^{32}S_2^{2-})]^{2+}$ (**2**-^{32}S) is high for a S_2^{2-} moiety, reflecting the strong interaction between the S_2^{2-} and Cu^{II} ion centers, which removes electron density from the S−S π^*_σ orbital and leads to a strengthened S−S bond.[46] Complex **2** has additional Raman peaks at 258, 650, and 1021 cm^{-1} (Figure 4), which are assigned as $\nu(Cu-N)_{py}$ vibrations, an internal pyridine ring mode, and an internal ligand mode, respectively. The two additional Raman peaks, observed at 409 and 452 cm^{-1}, are the result of a Fermi doublet and a fit of the energy splitting and resonance intensity results in the assignment of the $\nu(Cu-N)_{amine}$ stretch at 443 cm^{-1}.[11,47]

Reversible Sulfur Binding to [(TMPA′)$Cu^I]^+$ (1). Dioxygen binding to [(**TMPA**)$Cu^I(CH_3CN)]^+$ (**3**) and many other ligand−copper(I) or dicopper(I) complexes, synthetic[48−50] and of course biological (i.e., the O_2 carrier protein hemocyanin),[51,52] is reversible. We find that by varying the temperature of solutions of [{(**TMPA′**)$Cu^{II}\}_2(\mu$-1,2-$S_2^{2-})]^{2+}$ (**2**), we can nicely demon-

(43) Isolation of a solid material, complex **2**, would of course have been desirable to confirm purity by mass spectrometry, elemental analysis, or a variety of spectroscopic techniques. We attempted many times to isolate a solid but without success because of thermal sensitivity and instability of complex **2**; it is a reversible sulfur binder and readily loses sulfur with attempts to force a precipitation. Electrospray ionization mass spectrometric measurements on cold solutions of **2** give a signal corresponding only to [(TMPA′)$Cu^I]^+$, indicating loss of sulfur and reduction.

(44) Resonance Raman spectra for complex **4** (ref 11) also show evidence for a Fermi resonance of ν(S−S) with a local non-enhanced mode. Analysis of the data in ref 11 using the model in Figure 5 gives unmixed modal energies of the ^{32}S and ^{34}S ν(S−S) stretches of complex **4** to be 493 and 485 cm^{-1}, very similar to those of complex **2**.

(45) Skulan, A. J.; Hanson, M. A.; Hsu, H.-f.; Que, L., Jr.; Solomon, E. I. *J. Am. Chem. Soc.* **2003**, *125*, 7344−7356.
(46) Müller, A.; Jaegermann, W.; Enemark, J. H. *Coord. Chem. Rev.* **1982**, *46*, 245−280.
(47) Baldwin, M. J.; Ross, P. K.; Pate, J. E.; Tyeklár, Z.; Karlin, K. D.; Solomon, E. I. *J. Am. Chem. Soc.* **1991**, *113*, 8671−8679.
(48) Quant Hatcher, L.; Karlin, K. D. *J. Biol. Inorg. Chem.* **2004**, *9*, 669−683.
(49) Lewis, E. A.; Tolman, W. B. *Chem. Rev.* **2004**, *104*, 1047−1076.
(50) Mirica, L. M.; Ottenwaelder, X.; Stack, T. D. P. *Chem. Rev.* **2004**, *104*, 1013−1045.
(51) Kurtz, D. M., Jr. Dioxygen-Binding Proteins. In *Bio-coordination Chemistry;* Que, L., Jr., Tolman, W. B., Eds.; Elsevier: Oxford, 2004; Vol. 8, pp 229−260.
(52) Solomon, E. I.; Sundaram, U. M.; Machonkin, T. E. *Chem. Rev.* **1996**, *96*, 2563−2605.

strate that the binding of the disulfur moiety to **1** is reversible. Heating/cooling cycles on solutions of **2** could be easily carried out. That elemental sulfur is released from a warmed (to RT) −80 °C solution of **2** (Cu/S = 1:1) is evident from the fact that no sulfur from outside needs to be added to fully reform the purple solution upon recooling (see Supporting Information, Figure S4, for a cycling experiment carried out by spectrophotometric monitoring). This disulfide formation/desulfurization/sulfurization cycle can be repeated multiple times without addition of more S_8 or absorbance intensity loss. The following paragraphs show that the dioxygen reactivity of $[(\mathbf{TMPA'})Cu^{I}]^{+}$ (**1**) is not similarly reversible.

Reaction Chemistry of $[\{(\mathbf{TMPA'})Cu^{II}\}_2(\mu\text{-}1,2\text{-}S_2^{2-})]^{2+}$ (2). The primary goal of the work was to generate a *pure* end-on bound disulfido−dicopper(II) complex to probe the chemical nature of the coordinated disulfur moiety. Such comparisons have been important in copper−dioxygen chemistry (i.e., observing different chemical behaviors for end-on and side-on peroxodicopper(II) complexes).[48,53] Until now, only side-on disulfido−dicopper(II) complex reactivity has been probed.[7] Key issues are the effect of the N-ligand denticity, which, as will be seen, seems to control the disulfur-binding mode, the coordinated chalcogen reactivity, and whether the nature of the reactivity is electrophilic or nucleophilic in its character.

Previously, we reported the reactivity of $[\{(N_3)Cu^{II}\}_2(\mu\text{-}\eta^2\text{:}\eta^2\text{-}S_2^{2-})]^{2+}$ (**5**), a structurally characterized (Chart 2) side-on disulfido−dicopper(II) complex, with PPh_3, 2,6-dimethylisocyanide, carbon monoxide, dioxygen, **TMPA**, and benzyl bromide.[7] For example, the reaction of **5** with PPh_3 leads to nearly quantitative yields of $S{=}PPh_3$, while with excess (4 equiv) PPh_3, the copper(I) is trapped as the phosphine adduct/complex $[(N_3)Cu^{I}(PPh_3)]^{+}$. Sulfur from disulfide moiety of **5** can also be transferred to 2,6-dimethylisocyanide to form the corresponding isothiocyanate.[54] Interestingly, there is no reaction of **5** with benzyl bromide. This latter $PhCH_2Br$ reactivity, combined with the results of the PPh_3, indicates that the disulfur moiety in **5** is electrophilic.[7]

Thus, we subjected $[\{(\mathbf{TMPA'})Cu^{II}\}_2(\mu\text{-}1,2\text{-}S_2^{2-})]^{2+}$ (**2**), an end-on bound dicopper disulfide, to those same reagents (Scheme 2) to probe as well as to compare and contrast the nature of Cu_2S_2 species formed with the tetradentate chelate **TMPA′**.

Reaction of 2 with CO: Displacement of Disulfur Moiety/CO Reversibility. An additional indication that solutions of $[\{(\mathbf{TMPA'})Cu^{II}\}_2(\mu\text{-}1,2\text{-}S_2^{2-})]^{2+}$ (**2**) bind sulfur reversibly comes from the observation that carbon monoxide can displace sulfur (Scheme 2).[54] Bubbling CO through a −80 °C solution bleaches the purple color because of **2**, and $[(\mathbf{TMPA'})Cu^{I}(CO)]^{+}$ (**8**), the corresponding carbonyl adduct, is formed. Complex **8**, which could be isolated as a solid, has been characterized by elemental analysis, ^1H NMR, and IR spectroscopy (see Experimental Section). Its observed ν_{CO} value (=2094 cm^{-1}) is typical for that found with other **TMPA** analogues (ν_{CO} = 2091−2094 cm^{-1})[55] and suggests an overall five-coordinate ($Cu^{I}N_4(CO)$) structure (at least as a solid).[56] However, application of a vacuum/argon purge removes CO from the reaction solutions and leads to a reformation of purple species **2**, as followed by UV−vis spectroscopy (Figure 6 and Scheme 2). That elemental sulfur must be reformed in the reaction of **2** with CO is indicated by the reversible nature of the reaction. This carbonylation/sulfur-release/CO-removal cycle can be repeated several times.

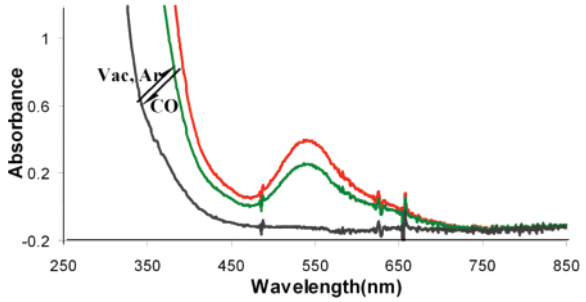

Figure 6. UV−vis spectra at −80 °C in THF, illustrating formation of the end-on disulfide complex $[\{(\mathbf{TMPA'})Cu^{II}\}_2(\mu\text{-}1,2\text{-}S_2^{2-})]^{2+}$ (**2**) from $[(\mathbf{TMPA'})Cu^{I}]^{+}$ (**1**)/S_8 reactivity (red spectrum), followed by generation of $[(\mathbf{TMPA'})Cu^{I}(CO)]^{+}$ (**8**) (black) upon CO bubbling through this solution of **2**. The green spectrum shown (of **2**) resulted following three argon/CO reaction cycles.

Reaction of 2 with TMPA: Ligand Exchange Reaction/Disulfide Transfer. Evidence for the presence of the Cu_2S_2 moiety in $[\{(\mathbf{TMPA'})Cu^{II}\}_2(\mu\text{-}1,2\text{-}S_2^{2-})]^{2+}$ (**2**) and its dynamic behavior also comes from its reaction (Scheme 2) with an anaerobic THF solution of **TMPA** (1.1 equiv to excess), the ligand present in the X-ray structurally characterized complex $[\{(\mathbf{TMPA})Cu^{II}\}_2(\mu\text{-}1,2\text{-}S_2^{2-})]^{2+}$ (**4**). The result is a color change from purple to deep blue, leading to an absorption spectrum that is identical to that observed for solutions from $[(\mathbf{TMPA})Cu^{I}(CH_3CN)]^{+}$ (**3**)/S_8 reactivity (Figure 3A). Thus, a ligand exchange (or perhaps a {Cu−(S_2)−Cu} exchange) occurs, also indicating that disulfido−dicopper(II) complex(es) with the **TMPA** ligand are more stable (thermodynamically) than **2** itself. This indicates a decrease in the chelating strength for copper(II) species of **TMPA** derivatives which possess 6-substitution at one of the pyridine ring; such 6-pyridyl substituents are anyways known to lead to geometric distortions from trigonal bipyramidal.[29]

We note that Tolman and co-workers have described a related exchange reaction where a side-on bound $\mu\text{-}\eta^2\text{:}\eta^2\text{-}S_2^{2-}$−dicopper(II) species reacts with a separate copper(I) complex with slightly different ligand (L′) and a disulfide exchange occurs; a disulfido−dicopper(II) complex with L′ now forms.[10] We also observed that the side-on bound disulfide complex $[\{(N_3)Cu^{II}\}_2(\mu\text{-}\eta^2\text{:}\eta^2\text{-}S_2^{2-})]^{2+}$ (**5**)[7] reacts with **TMPA**, leading to a net displacement of the tridentate N_3 ligand, giving $[\{(\mathbf{TMPA})Cu^{II}\}_2(\mu\text{-}1,2\text{-}S_2^{2-})]^{2+}$ (**4**) (and the complexes in equilibrium with it, see above).[7] The combined observations suggest copper(II) complexes with disulfide ligands are labile and possess a dynamic behavior.

Reaction of $[(\mathbf{TMPA'})Cu^{I}]^{+}$ (1) and $[\{(\mathbf{TMPA'})Cu^{II}\}_2(\mu\text{-}1,2\text{-}S_2^{2-})]^{2+}$ (2) with O_2: Formation of $[\{(\mathbf{TMPA'})Cu^{II}\}_2(\mu\text{-}1,2\text{-}O_2^{2-})]^{2+}$ (9). A THF solution of **1** at −80 °C reacts with

(53) Paul, P. P.; Tyeklár, Z.; Jacobson, R. R.; Karlin, K. D. *J. Am. Chem. Soc.* **1991**, *113*, 5322−5332.
(54) By contrast, Tolman and coworkers[15] find somewhat differing reactivity of side-on bound $Cu^{II}_2(S_2^{2-})$ complexes with anilido−imine ligand. For example, reaction with isocyanide gives a Cu(I)−NCR complex and without sulfur transfer. There is also a contrast in reaction of the disulfide species with 2 equiv of PPh_3, in their case giving a 1:1 mixture of $S{=}PPh_3$ and Cu(I)−PPh_3, along with unreacted $Cu^{II}_2(S_2^{2-})$ complex. With dioxygen and CO, there is a complete lack of reactivity.
(55) Zhang, C. X.; Kaderli, S.; Costas, M.; Kim, E.-i.; Neuhold, Y.-M.; Karlin, K. D.; Zuberbühler, A. D. *Inorg. Chem.* **2003**, *42*, 1807−1824.
(56) Kretzer, R. M.; Ghiladi, R. A.; Lebeau, E. L.; Liang, H.-C.; Karlin, K. D. *Inorg. Chem.* **2003**, *42*, 3016−3025.

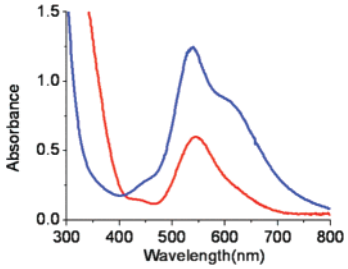

Figure 7. UV−vis spectra of [{(**TMPA′**)Cu^{II}}$_2$(μ-1,2-S_2^{2-})]$^{2+}$ (**2**) (red) at −124 °C in MeTHF and formation of end-on peroxide species [{(**TMPA′**)Cu^{II}}$_2$(μ-1,2-O_2)]$^{2+}$ (**9**) (blue) upon bubbling the solution with O_2.

O_2, leading to a purple solution with prominent UV−vis features at λ_{max} = 540 nm (ϵ, 9550 M^{-1} cm^{-1}) and 610 nm, sh (ϵ, 6500 M^{-1} cm^{-1}) (see Supporting Information, Figure S6).[54] These spectral features, both absorption maxima and absorptivity (ϵ) values, are characteristic of known μ-1,2-peroxodicopper(II) complexes, including that for the well described (with X-ray structure) complex [{(**TMPA**)Cu^{II}}$_2$(μ-1,2-O_2^{2-})]$^{2+}$ (**10**).[31,47,48,50] Given the established nature of such species in a ligand framework **TMPA′** so similar to that of **TMPA**, we can confidently conclude that **9** is a μ-1,2-peroxodicopper(II) complex, a close analogue of **10**. This reaction of **1** with O_2 at −80 °C is immediate (by benchtop monitoring), and the binding of O_2 appears to be irreversible, as warming does not lead to release of O_2 and regeneration of **1**.

Most interestingly, bubbling O_2 through −124 °C MeTHF solutions of the disulfido−dicopper(II) complex **2** leads to a rapid spectral change indicating that [{(**TMPA′**)Cu^{II}}$_2$(μ-1,2-O_2^{2-})]$^{2+}$ (**9**), λ_{max} = 540 nm (Scheme 2, Figure 7), is formed. The absorptivity of this product solution (Figure 7) indicates that a quantitative conversion of **2** to **9** occurs; thus, we can conclude that sulfur is not oxidized during this disulfide complex oxygenation process. This "disulfide (or sulfur) displacement" reaction is attributed to the lability of the Cu_2S_2 moiety.

Reaction of [{(TMPA′)Cu^{II}}$_2$(μ-1,2-S_2^{2-})]$^{2+}$ (2) with PPh_3. Triphenylphosphine is a good ligand for copper(I) complexes,[31,57] and we have also used it to establish reactivity patterns for copper−dioxygen adducts.[48,53] More recently, we studied reactions of our μ-η^2:η^2-S_2^{2-}−dicopper(II) [{(N_3)Cu^{II}}$_2$-(μ-η^2:η^2-S_2^{2-})]$^{2+}$ (**5**) (Chart 2).[7,54] Here, comparison of the reaction behavior of PPh_3 with **2** versus **5**[7] indicates a noticeably *less* electrophilic disulfur unit present in **2**. Four equiv of PPh_3 were reacted with **2** with the result that a Cu(I)−PPh_3 complex [(**TMPA′**)Cu^{I}(PPh_3)]$^{+}$ (**11**) was isolated and sulfur ended up "trapped" by PPh_3 giving S═PPh_3 (Scheme 2). The reaction proceeded according to eq 2, with near quantitative yields of both products being formed (see Experimental Section).

$$[\{(\mathbf{TMPA'})Cu^{II}\}_2(\mu\text{-}1,2\text{-}S_2^{2-})]^{2+}\ (\mathbf{2}) + 4PPh_3 \rightarrow 2[(\mathbf{TMPA'})Cu^{I}(PPh_3)]^{+}\ (\mathbf{11}) + 2S{=}PPh_3 \quad (2)$$

Note that we previously showed that PPh_3 reacts with the peroxo complex [{(**TMPA**)Cu^{II}}$_2$(μ-1,2-O_2^{2-})]$^{2+}$ (**10**) to release all the O_2 and give [(**TMPA**)Cu^{I}(PPh_3)]$^{+}$;[31,53] the difference here is that PPh_3 reacts with elemental sulfur as well. Thus, we suggest that PPh_3 reaction with **2** leads to release of elemental sulfur with formation of both [(**TMPA′**)Cu^{I}(PPh_3)]$^{+}$ (**11**) and S═PPh_3 driving the reaction.

Addition of 2 equiv of PPh_3 (not an excess) to **2** gives an ∼1:1 mixture of adduct [(**TMPA′**)Cu^{I}(PPh_3)]$^{+}$ (**11**) and S═PPh_3 (see Experimental Section). We wish to contrast this with the observation that reaction of 2 equiv of PPh_3 with side-on bound disulfido−dicopper(II) complex [{(N_3)Cu^{II}}$_2$(μ-η^2:η^2-S_2^{2-})]$^{2+}$ (**5**) gives *complete* conversion of all the PPh_3 present to S═PPh_3,[7] suggesting the disulfur moiety bound to copper(II) ion in **2** is less electrophilic in its reaction with PPh_3.

Reactions of disulfido or sulfido−metal complexes with PPh_3 often give S═PPh_3.[4] Thus, [{Co(Salphen)}$_2$$S_2$Na(THF)$_2$]$BPh_4$ and $Mo^{VI}O(\eta^2$-$S_2)(S_2CNR_2)_2$ disulfur complexes react with PPh_3 to form corresponding reduced metal complexes [{Co(Salphen)}$_2$Na(THF)$_2$]BPh_4[58] and $Mo^{IV}O(S_2CNR_2)_2$,[59] respectively, along with the formation of S═PPh_3. Sulfur transfer reactions to PPh_3 are also observed with other metal−sulfide complexes (e.g., for $MeRe^{VII}O_2S$,[60] [HB(3,5-Me_2pz)$_3$]W^{VI}(S)-Cl),[61] leading to $MeRe^{V}O_2$ and [HB(3,5-Me_2pz)$_3$]W^{IV}S(solv)-Cl, respectively, along with S═PPh_3 in each case.[4]

Reaction of [{(TMPA′)Cu^{II}}$_2$(μ-1,2-S_2^{2-})]$^{2+}$ (2) with ArN≡C: Sulfur Transfer and Isolation of [(TMPA′)Cu^{I}-(C≡NAr)]$^{+}$ (12). Activation and utilization of elemental sulfur to synthesize organosulfur compounds are of general interest,[62−64] with one example being the transfer of sulfur to an isocyanide to give an isothiocyanate.[63] Reaction of 4 equiv of 2,6-dimethylphenyl isocyanide (ArN≡C) with **2** resulted in facile sulfur atom transfer to form 2,6-dimethylphenyl isothiocyanate (ArNCS; 85% yield) (Scheme 2) and the pale yellow copper(I) complex [(**TMPA′**)Cu^{I}(C≡NAr)]$^{+}$ (**12**) (70% yield; ν(N≡C) = 2140 cm^{-1}; see Experimental Section).[54] We have previously synthesized and characterized nitrogen ligand copper(I)−isocyanide complexes, for example, [Cu^{I}(Me_2Im)$_2$(C≡NAr)]$^{+}$ {Me_2Im = 1,2-dimethylimidazole; ν(N≡C) = 2116 (solid), 2124 (MeOH−H_2O solution) cm^{-1}}[65] and [Cu^{I}(MePY2)-(C≡NAr)]$^{+}$ {MePY2 = bis(2-pyridylethyl)methylamine; ν(N≡C) = 2132 ($CHCl_3$ solution) cm^{-1}},[66] and Floriani and co-workers[67] previously described a number of cuprous isocyanide complexes. The active site of cuprous proteins has also been probed using isocyanide as a copper(I) specific ligand.[65,66]

Thus, the reaction of ArN≡C with **2** is similar to the behavior observed for PPh_3 (see above) which led to net sulfur atom transfer along with reagent (ArN≡C or PPh_3) stabilization and complexation of copper(I). Isocyanide (ArN≡C) reaction with the side-on disulfido−dicopper(II) complex [{(N_3)Cu^{II}}$_2$(μ-η^2:η^2-S_2^{2-})]$^{2+}$ (**5**) also led to the efficient generation of isothiocyanate.[7]

(57) Jardine, F. H. *Adv. Inorg. Chem. Radiochem.* **1975**, *17*, 115−163.
(58) Floriani, C.; Fiallo, M.; Chiesivilla, A.; Guastini, C. *J. Chem. Soc., Dalton Trans.* **1987**, 1367−1376.
(59) Leonard, K.; Plute, K.; Haltiwanger, R. C.; Dubois, M. R. *Inorg. Chem.* **1979**, *18*, 3246−3251.
(60) Jacob, J.; Espenson, J. H. *Chem. Commun.* **1999**, 1003−1004.
(61) Eagle, A. A.; Gable, R. W.; Thomas, S.; Sproules, S. A.; Young, C. G. *Polyhedron* **2004**, *23*, 385−394.
(62) Matsumoto, K.; Sugiyama, H. *J. Organomet. Chem.* **2004**, *689*, 4564−4575.
(63) Arisawa, M.; Ashikawa, M.; Suwa, A.; Yamaguchi, M. *Tetrahedron Lett.* **2005**, *46*, 1727−1729.
(64) Adam, W.; Bargon, R. M. *Chem. Rev.* **2004**, *104*, 251−261.
(65) Rhames, F. C.; Murthy, N. N.; Karlin, K. D.; Blackburn, N. J. *J. Biol. Inorg. Chem.* **2001**, *6*, 567−577.
(66) Reedy, B. J.; Murthy, N. N.; Karlin, K. D.; Blackburn, N. J. *J. Am. Chem. Soc.* **1995**, *117*, 9826−9831.
(67) Toth, A.; Floriani, C.; Chiesivilla, A.; Guastini, C. *J. Chem. Soc., Dalton Trans.* **1988**, 1599−1605.

Reaction of [{(TMPA′)Cu^{II}}$_2$(μ-1,2-S$_2^{2-}$)]$^{2+}$ (2) with PhCH$_2$Br: Formation of Dibenzyl Disulfide. A most informative observation is the reaction of benzyl bromide (Scheme 2) with [{(**TMPA′**)Cu^{II}}$_2$(μ-1,2-S$_2^{2-}$)]$^{2+}$ (**2**), compared to the behavior observed with side-on bound [{(N$_3$)Cu^{II}}$_2$(μ-η^2:η^2-S$_2^{2-}$)]$^{2+}$ (**5**), where in fact there is *no* reaction.[7]

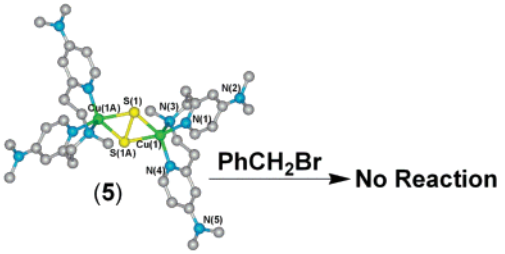

Addition of PhCH$_2$Br to **2** under anaerobic conditions is accompanied by a change in color from purple to green. Isolation and characterization of the metal complex product show it to be the green copper(II) complex, [{(**TMPA′**)Cu^{II}(Br)}$_2$](B(C$_6$F$_5$)$_4$)$_2$ (**6**), confirmed by elemental analysis and comparison of UV−vis and IR spectroscopic data which match those of the compound obtained by reaction of [(**TMPA′**)Cu^{I}]$^{+}$ (**1**) with CHBr$_3$ as described above (see Experimental Section and Supporting Information, Figures S2 and S3). Concomitant formation of the organic product dibenzyldisulfide (PhCH$_2$SSCH$_2$Ph) (Scheme 2) in ∼70% yield was confirmed by GC and GC−MS spectrometry (see Experimental Section). The reaction of **2** with PhCH$_2$Br illustrates the *nucleophilic* nature of the end-on bound disulfur moiety in the Cu$_2$S$_2$ core of **2**, contrasting directly with that observed for the side-on bound disulfide moiety in **5**, which is *unreactive* toward benzyl bromide (diagram above). Interestingly, small amounts of the sulfide and trisulfide products PhCH$_2$SCH$_2$Ph and PhCH$_2$SSSCH$_2$Ph also form during PhCH$_2$Br reactivity with **2**, in ∼10 and ∼15% yields, respectively. A related reaction of PhCH$_2$Br, but with a solution derived from a [(**TMPA**)Cu^{I}(CH$_3$CN)]$^{+}$ (**3**)/(0.37)S$_8$ reaction, reveals that the formation of PhCH$_2$SSCH$_2$Ph, PhCH$_2$SCH$_2$Ph, and PhCH$_2$SSSCH$_2$Ph occurs in yields of 12, 5, and 75%, respectively. The contrasting behavior of **2** and **4** (mixtures in this latter case) shows that the solution containing [{(**TMPA**)Cu^{II}}$_2$(μ-1,2-S$_2^{2-}$)]$^{2+}$ (**4**) apparently does *not* equilibrate to react only as a μ-1,2-disulfido complex (like the X-ray structure, Chart 1). That solutions of **4** give a product distribution completely different from that of reaction of PhCH$_2$Br with **2** is also consistent with the earlier stipulation that solutions of [{(**TMPA′**)Cu^{II}}$_2$(μ-1,2-S$_2^{2-}$)]$^{2+}$ (**2**) consist of only the one disulfido species. The origin of the sulfide and trisulfide organics is not clear; future research will be needed to sort out how these might originate from more complex transformations starting from **2** + PhCH$_2$Br.

To our knowledge, there are no examples of a disulfide such as PhCH$_2$SSCH$_2$Ph forming from the reaction of a metal disulfide complex with an electrophile such as PhCH$_2$Br. Analogous reactions do occur when PhCH$_2$Br is exposed to the platinum peroxo complex Pt(PPh$_3$)$_2$(O$_2$); initially, an alkylperoxo complex Pt(PPh$_3$)$_2$(OOCH$_2$Ph)Br is formed, and this further reacts with another molecule of benzyl bromide to produce Pt(PPh$_3$)$_2$Br$_2$ and benzyl peroxide (PhCH$_2$OOCH$_2$Ph).[68] In a related reaction, Ni(*t*-BuNC)$_2$O$_2$ reacts with 2 equiv of trityl cation resulting in the formation of trityl peroxide, Ni(*t*-BuNC)$_2$(O$_2$) + 2 Ph$_3$CX → Ni(*t*-BuNC)$_2$X$_2$ + Ph$_3$COOCPh$_3$ (X = Br, BF$_4$).[69] Thus, the formation of PhCH$_2$SSCH$_2$Ph from disulfido−dicopper(II) complex [{(**TMPA′**)Cu^{II}}$_2$(μ-1,2-S$_2^{2-}$)]$^{2+}$ (**2**) parallels the reaction of certain *nucleophilic* metal−dioxygen complexes[70] with PhCH$_2$Br, where PhCH$_2$OOCH$_2$Ph forms.

Summary and Conclusions

The present study, along with our previous investigation of [{(N$_3$)Cu^{II}}$_2$(μ-η^2:η^2-S$_2^{2-}$)]$^{2+}$ (**5**),[7] shows that end-on bound Cu$_2$S$_2$ species [{(**TMPA′**)Cu^{II}}$_2$(μ-1,2-S$_2^{2-}$)]$^{2+}$ (**2**) possesses a nucleophilic disulfur moiety, whereas the side-on ligated disulfur Cu$_2$S$_2$ moiety is electrophilic in nature. Thus, ligand-Cu^{I}/S$_8$ reactivity appears to parallel known ligand-Cu^{I}/O$_2$ chemistry, as side-on bound peroxo dicopper(II) complexes are generally electrophilic compared to end-on bound peroxides (e.g., as with **TMPA**), which are nucleophilic toward exogenous substrates.[48,53] These new structural and functional findings give a picture of the diversity of copper−sulfur chemistry and reemphasize the key role the ligand (e.g., denticity) plays in structure and reactivity.[48,71] Future copper−sulfur studies will continue to explore and find new structures and reactivity patterns while also employing these tetradentate and tridentate ligated Cu$_2$S$_2$ complexes as synthons in the generation and synthesis of structure and functional models for N$_2$OR.

Acknowledgment. This work was supported by grants from the National Institutes of Health (K.D.K., GM28962; E.I.S., DK31450).

Supporting Information Available: X-ray structure selected bond lengths and angles, UV−vis, IR, and resonance Raman spectroscopic details, and CIF files. This material is available free of charge via the Internet at http://pubs.acs.org.

JA071968Z

(68) Tatsuno, Y.; Otsuka, S. *J. Am. Chem. Soc.* **1981**, *103*, 5832−5839.
(69) Otsuka, S.; Nakamura, A.; Tatsuno, Y.; Miki, M. *J. Am. Chem. Soc.* **1972**, *94*, 3761−3767.
(70) Sheldon, R. A.; Kochi, J. K. *Metal-Catalyzed Oxidations of Organic Compounds;* Academic Press: New York, 1981.
(71) Hatcher, L. Q.; Karlin, K. D. *Adv. Inorg. Chem.* **2006**, *58*, 131−184.